



Bulletin of the Mineral Research and Exploration

<http://bulletin.mta.gov.tr>



An overview of the current seismicity of the Sultandağı Fault Zone (Afyonkarahisar-Konya, Western Anatolia)

Doğan KALAFAT^{a*}, Yavuz GÜNEŞ^a, Mehmet KARA^a and Kıvanç KEKOVALI^a

^aKandilli Observatory and Earthquake Research Institute, RETMC, Boğaziçi University, İstanbul, Turkey

Research Article

Keywords:

Western Anatolia,
Sultandağı Fault Zone,
Micro-earthquake,
Seismic network, Digital
broadband earthquake
stations

ABSTRACT

Western Anatolia is one of the most seismically active regions in Turkey. The high seismic activity is a result of a complex tectonic deformation dominated by the N-S extensional tectonic regime in Western Anatolia. This tectonic deformation is also a result of the relative movement of the African-Arabian plates towards the north, which causes the Anatolian plate to shift 2.5 cm per year towards W-SW. One of the largest fault zones in the Western Anatolia, Sultandağı Fault Zone (SFZ) has a northwest-southeast trend. SFZ, approximately 120 km long, is an important tectonic structure, which produced three major earthquakes ($M_w > 6.0$) between the years of 2000 -2002. Therefore, the most significant goals of this study were to monitor the micro-earthquakes along SFZ, to enrich the current seismic network and to increase the earthquake detection threshold in the region ($M_c < 2.5$). Within the scope of the study, 3 digital broadband earthquake stations were installed in the region. The analysis of the data obtained in the research indicated that the central and western parts of SFZ are active and there is intense seismic activity especially in the vicinity of Sultandağı, Çay, Çobanlar, and Afyonkarahisar. Fault plane solutions revealed that the earthquakes in the region generally occur with normal faulting with oblique components. Seismic stations installed within the scope of the study contributed positively to the increase of the sensitivity ($M_c = 1.3$) of the earthquake detection threshold (M_c) in the region and increased the detection capacity.

Received Date: 05.12.2019

Accepted Date: 13.04.2020

1. Introduction

Sultandağı Fault Zone (SFZ) is one of the most important tectonic structures in Western Anatolia and has produced 3 important earthquakes in the last two decades (Figure 1). Between the years 2000 and 2002, 3 major earthquakes ($M_w > 6.0$) occurred on the Sultandağı Fault Zone, also called as Afyon-Akşehir Graben. The first earthquake (Eber-Sultandağı earthquake $M_w = 6.0$) occurred in 2000, followed by the Sultandağı ($M_w 6.5$) and Çay-Sultandağı earthquakes ($M_w = 6.0$) on February 3, 2002.

The last two earthquakes occurred consecutively on the Sultandağı Fault Zone (SFZ) on the same day, and the main shocks were followed by extensive aftershock activity. In this context, seismic activity in the form of an earthquake series in the region in recent years has revealed that the faults around the northwestern end of SFZ, especially the ones around Çay-Sultandağı-Afyonkarahisar, are each an active fault segment that can be considered within this fault zone. NW-SE and NE-SW trending faults play an important role in the tectonic development of the region. This makes it necessary to monitor regularly and precisely both the micro-earthquake activity and

Citation info: Kalafat, D., Güneş, Y., Kara, M., Kekovalı, K. 2020. An overview of the current seismicity of the Sultandağı Fault Zone (Afyonkarahisar-Konya, Western Anatolia). Bulletin of the Mineral Research and Exploration 163, 187-210.
<https://doi.org/10.19111/bulletinofmre.721796>

*Corresponding author: Doğan KALAFAT, kalafato@boun.edu.tr



Figure 1- Study Area (Sultandağı Fault Zone), active fault zones and major tectonic plates across and in the vicinity of Turkey (active faults were taken from Emre et al., 2013; the figure was drawn using the GMT software; topography data was obtained from NASA-SRTM).

the recent earthquake activity which continues as series of earthquakes. The fact that the seismic stations in the region were not sufficient before the study, and, therefore, that the current seismic activity could not be followed properly made up the key motivational elements for the necessity to conduct a study in the region.

Therefore, monitoring the micro-earthquakes along SFZ, enriching the current seismic network and increasing the earthquake detection threshold in the region ($M_c < 2.5$) were the most important goals of this study.

2. General Geological Structure and Seismicity

The region is under the influence of the extension regime which is dominant in Western Anatolia, and earthquake activity occurs as a result of this extension regime. However, this region, known as Turkish Lake District or Isparta Bend, where the Central and Western Taurus Mountains meet, contains different

rock groups in terms of stratigraphic and structural features. Therefore, there are two basic views regarding the neotectonic regime of the region. The first one is that it is a compression regime, which is suggested by various researchers (Boray et al., 1985; Barka et al., 1995; Uysal, 1995; Altunel et al., 1999). In the second one, it is argued that no compression tectonic regime has occurred in Isparta Bending after the early Messinian (upper Miocene) compression deformation phase, and that the neotectonic regime in Isparta Bending is extensional (Koçyiğit, 1996; Glover and Robertson, 1998; Koçyiğit and Özacar, 2003).

Turkish Lake District is roughly bordered by Denizli, Fethiye, Antalya, Alanya, Akseki, Ahırılı, Seydişehir, Beyşehir, Afyon, Sandıklı and Çivril. This section generally consists of many blocks of different sizes which are located between NE-SW, NW-SE and N-W trending dip-slip normal faults (Figure 2). Some of them represent depression and some represent elevation areas. Compression stress concentrating in different directions along the edges of the Anatolian-

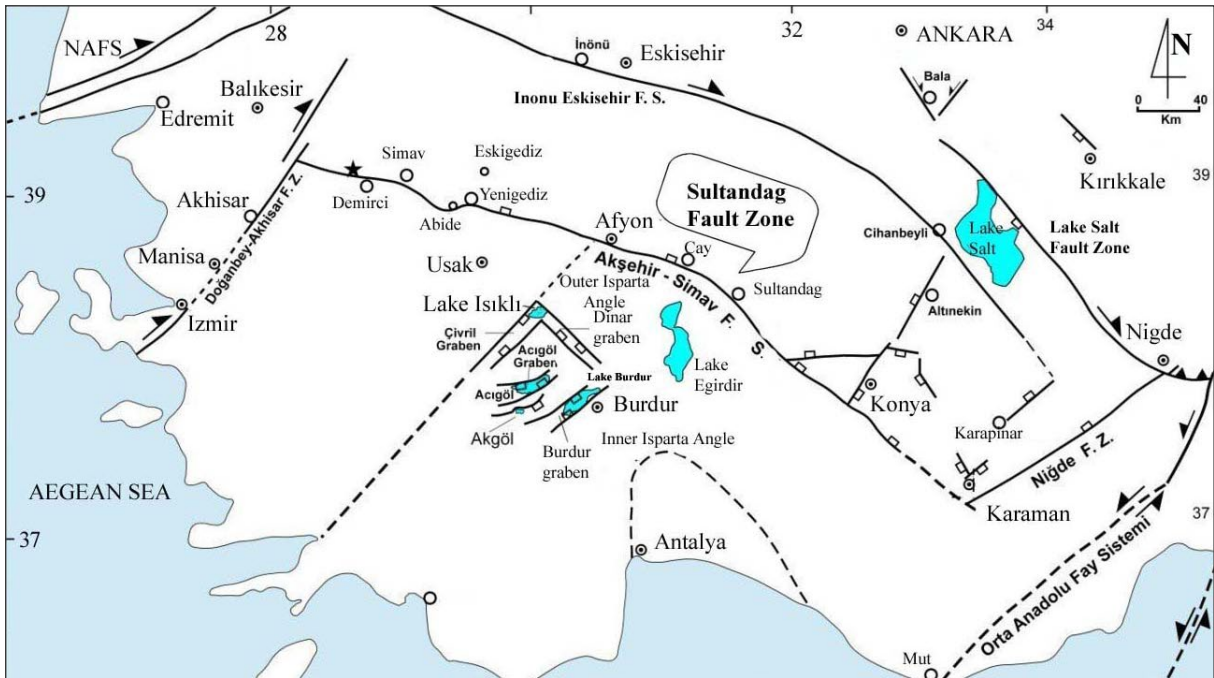


Figure 2 - Active tectonic elements in the region (taken from Koçyiğit, 2008; Akşehir-Simav Fault System, Dinar-Acıgöl-Burdur-Çivril Grabens: Normal Faults; Lake Salt FZ, İnönü Eskişehir FS, Middle Anatolian FS: Strike-Slip faults and between both systems a thrust fault).

Aegean plates was released in the form of tensional stress also in different directions in the inner shell, which led to the formation of the faults mentioned above (Koçyiğit, 1984; Şengör et al., 1985; Seyitoğlu and Scott, 1996; Kaya et al., 2014).

Turkish Lake District was significantly fragmented by dip-slip normal faults that had developed before the Neogene period and remained active throughout it (Koçyiğit, 2008; Özgül et al., 1991). It is also claimed that the region is dominated by a compression system that causes large thrust and lateral strike-slip movements (Boray et al., 1985; Barka et al., 1995; Uysal, 1995). However, it is considered that local releases and, accordingly, pull-apart basins may have developed in this compression system (Koçyiğit, 1984, 1996; Koçyiğit et al., 2000). Turkish Lake District, which has been controlled by block faultings (normal) since the late middle Oligocene, continues its tectonic activity under the control of normal block faulting (grabens), especially in the vicinity of Burdur-Dinar-Afyon-Akşehir (Koçyiğit, 2008; Koçyiğit and Özacar, 2003). Therefore, geological and geomorphological findings indicate Holocene activity along the Sultandağı Fault Zone (Atalay, 1975; Şaroğlu et al., 1987, 1992; Ögdüm et al., 1991; Koçyiğit et al., 2000).

The February 3, 2002 Earthquakes occurred at SFZ as a result of this tectonic activity (Kalafat and Öz, 2001; Emre et al., 2003). Blumenthal, 1963 described the Sultandağı Fault as a large normal fault at the top of Isparta Bend. This region is the southeastern part of the extensional tectonics of western Anatolia (Emre et al., 2003).

It is quite intense in terms of earthquake activity and significant earthquakes in the last century are listed below (Table 1).

The recent earthquakes in the region reveal that NW-SE and NE-SW trending faults cause the current seismic activity. It was mentioned in the Turkish Active Fault Map (Emre et al., 2013) published by the MTA in 2003 that the 2002 earthquake occurred on the Çay segment (Table 1, Event 9), defined as Afyon-Akşehir Graben, with an extension to the northwest. The previous earthquake happened on this fault system on 15 December, 2000 (Figure 3). The fault system causing earthquakes has been defined as Sultandağı fault zone by various researchers (Kalafat and Öz, 2001; Kalafat et al., 2002, 2003; Emre et al., 2002; Ulusay et al., 2002).

Table 1- Major Earthquakes in the region (1900-2002).

Date (D/M/Y)	Time (h/m)	Lat. (N°)	Lon (E°)	Intensity (Io-MSK)	Mag. (M)	Location	Event No.
03.10.1914	22:07	38.00	30.00	IX	6.9	Burdur	1
07.08.1925	06:46	37.40	30.50	VIII	5.9	Dinar-Afyon	2
19.07.1933	20:07	38.20	29.80	VIII	5.7	Çivril- Denizli	3
22.11.1963	20:26	37.20	29.70	VII	5.1	Tefenni-Burdur	4
12.05.1971	06:25	37.60	29.72	VIII	5.9	Burdur	5
29.07.1978	04:34	37.57	30.02	VII	5.0	Burdur	6
01.10.1995	15:57	38.11	30.05	VIII	6.1	Dinar-Afyon	7
15.12.2000	16:44	38.63	31.19	VII	5.8	Sultandağı-Afyon	8
03.02.2002	07:11	38.58	31.25	VII	6.4	Sultandağı-Afyon	9
03.02.2002	09:26	38.68	30.38	VII	5.6	Sultandağı- Afyon	10

Source: Eyidoğan et al., 1991; Kalafat, 1996; Kalafat et al., 2000.



Figure 3- Distribution of the outer centers of the 2000 and 2002 Earthquakes [Active faults were taken from Emre et al., 2013; (The figure was drawn with the GMT software; the topography data is from NASA-SRTM)].

Land observations showed that, in the 2002 earthquakes, the WNW-ESE trending fault had damaged and affected the villages and towns located in this direction, especially to the S-SW of Eber Lake. Maltepe, Çobanlar and nearby villages of Çay and Sultandağı districts are the most affected settlements (Figure 4). The surface ruptures caused by the earthquake were observed to the SW of Eber,

and generally between Çay and Maltepe Villages. The general direction of the surface rupture is N 80° W. The surface rupture is divided into two as Maltepe and Çay fault segments (Kalafat et al., 2002; Kalafat and Görgün, 2017; figure 4).

The general direction of the fractures dominantly varies as EW, NE-SW / NW-SE. Vertical strike ranges

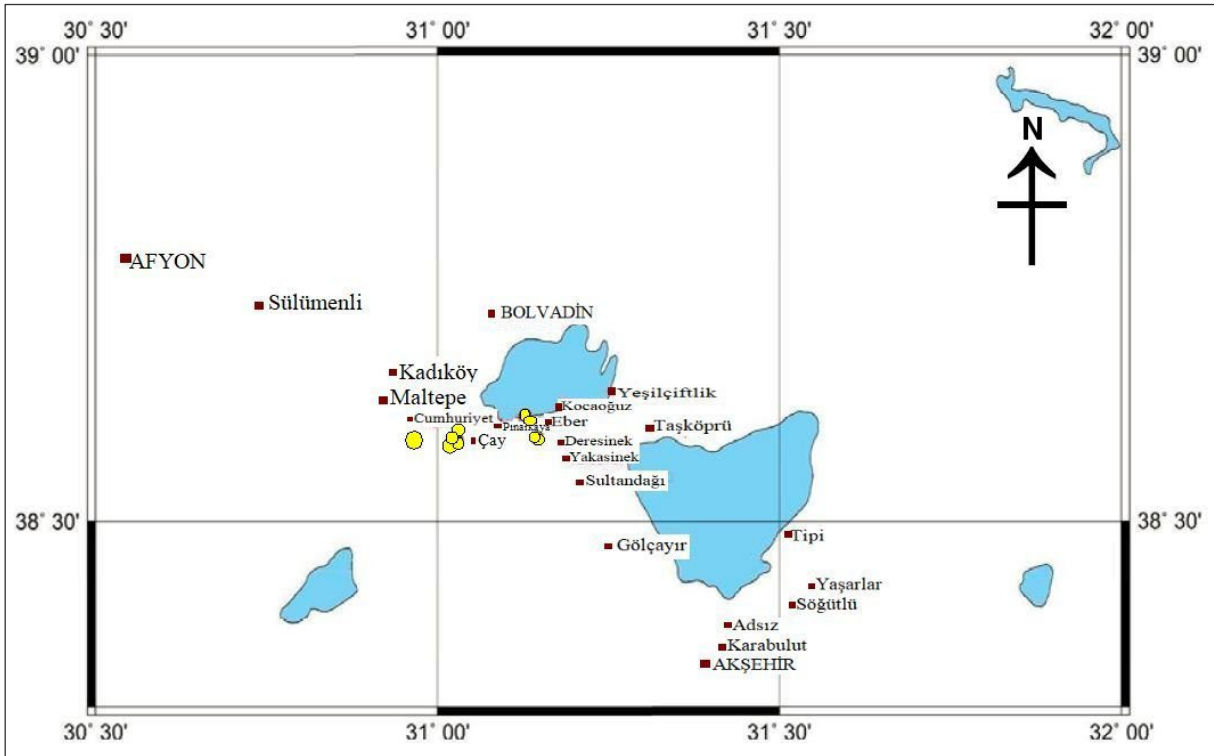


Figure 4- Locations of the surface ruptures and deformations (circles show the locations of the surface ruptures).

between 25 and 35 cm. The downthrown block is towards N-NE and the surface rupture resulting from the earthquake is approximately 18.5 (± 1.5) km (Kalafat et al., 2002; figure 5).

Various researchers supported these results, stating that the 2002 earthquakes caused a 26-km-surface rupture with a vertical displacement of up to 30 cm between Çay and Sultandağı and to the west of Çay (Emre et al., 2003; Akyüz et al., 2006). Emre et al (2003) stated that the rupture was 20 km long with

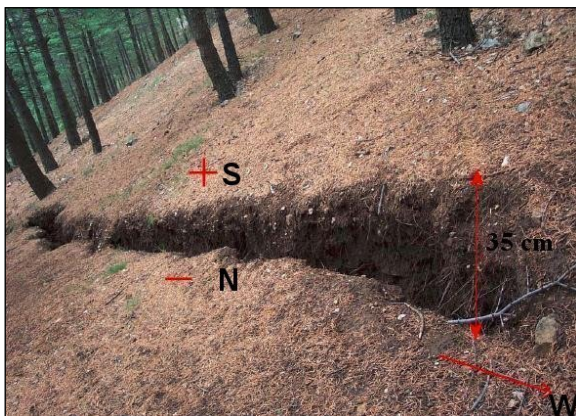


Figure 5- An example of surface ruptures observed in the field (Yaka district of Çay town; Kalafat et al., 2002).

a generally east-west trend and consisted of three distinct sections separated from each other, and that, during the earthquake, two conjugate normal surface faultings, called as Çay and Kali Çayı segments respectively, occurred.

The earthquake ($M_w = 6.0$) that occurred at 11:26 am, 2 hours after the main shock, was considered to be an earthquake and rupture which was triggered by the main shock (Kalafat et al., 2002). It hit the western part of Sultandağı fault, the area between Çay, Işıklar, and Çobanlar. Fault solutions revealed that earthquakes in the region generally occurred with oblique vertical strike normal faultings (Kalafat and Öz, 2001; Kalafat et al., 2002; Li et al., 2002; Kalafat and Görgün, 2017; figure 6, table 2).

The 3 February 2002 Sultandağı Earthquakes (Table 2, No=2-4) revealed that the earthquake activity continues in the region today under the influence of the extension regime. The extension regime is released by the formation of normal faults, which causes deformation and expansion. The Sultandağı earthquakes occurred as a result of the breaking of Sultandağı / Çay-Maltepe segments in the Sultandağı-Akşehir Fault system, stretching in a major E-W, NW-

Table 2- Fault Plane Solutions of important earthquakes in the region (1995-2019).

Eq. No.	Date G/A/Y	Time UTC	Lat. Deg.	Lon. Deg.	Depth. Km	Mag. Mw	FAULT PARAMETERS			REGION	Source
							Strike(°) Azimuth	Dip Angle	Rake Angle		
1	01.10.1995	15:57	38.06	29.68	15	6.4	310	60	-88	Dinar-Afyonkarahisar	HRV
2	15.12.2000	16:44	38.4	31.35	15	6	118	49	-81	Sultandağı-Afyonkarahisar	HRV
3	03.02.2002	07:11	38.62	31.21	15	6.5	66	55	-104	Sultandağı-Afyonkarahisar	HRV
4	03.02.2002	09:26	38.23	30.56	15	5.8	15	53	-118	Senirkent-Tatarlı-Isparta	HRV
5	03.02.2002	11:40	38.52	31.22	15	5.3	229	50	-108	Sultandağı-Afyonkarahisar	HRV
6	13.05.2002	11:42	38.59	31.12	5	4.3	288	88	-129	Eber-Çay-Afyonkarahisar	DK
7	26.06.2002	21:31	38.66	31.18	10	4.2	136	60	-105	Bolvadin-Afyonkarahisar	DK
8	05.08.2002	04:57	38.68	31.2	5	4.3	282	50	-113	Bolvadin-Afyonkarahisar	DK
9	03.07.2004	20:29	38.5	31.33	13	4.5	255	70	-85	Sultandağı-Afyonkarahisar	DK
10	08.08.2004	15:30	38.7	31.35	7	3.8	294	46	-116	Sultandağı-Afyonkarahisar	DK
11	07.09.2004	18:05	38.69	31.2	10	4.5	313	78	-32	Bolvadin-Afyonkarahisar	DK
12	16.09.2004	05:07	38.69	31.19	10	4.3	265	45	-65	Bolvadin-Afyonkarahisar	DK
13	08.11.2004	21:17	38.67	30.92	6	4.2	273	77	-76	Çay-Afyonkarahisar	DK
14	15.05.2005	10:54	38.61	30.78	6	4.2	296	43	-122	Çobanlar-Afyonkarahisar	DK
15	08.11.2006	12:09	38.59	30.75	10	3.3	334	33	-91	Kızıldağ-Afyonkarahisar	DK
16	19.04.2007	13:21	38.58	31.24	6	4	300	65	-60	Sultandağı-Afyonkarahisar	DK
17	06.05.2007	19:55	38.66	30.86	13	3.3	304	77	-39	Çay-Afyonkarahisar	DK
18	18.01.2009	19:39	38.81	31.4	15	3.5	218	74	-102	Emirdağ-Afyonkarahisar	DK
19	15.09.2009	09:54	38.71	31.28	7	3.5	230	35	-106	Bolvadin-Afyonkarahisar	DK
20	21.12.2009	21:09	38.68	31.21	10	3.7	225	32	-87	Bolvadin-Afyonkarahisar	DK
21	07.09.2013	23:59	38.45	30.63	16	3.9	300.2	36.4	-41.5	Şuhut-Afyonkarahisar	DK
22	28.11.2015	03:23	38.98	31.23	20	3.5	340	78	-89	Emirdağ-Afyonkarahisar	DK
23	18.10.2016	20:33	38.69	31.04	7	3.5	260	42	-74	Bolvadin-Afyonkarahisar	DK
24	18.10.2016	22:54	38.69	31.04	9	4.1	307	56	-32	Bolvadin-Afyonkarahisar	DK
25	08.08.2019	20:50	37.85	29.75	16	3.6	220	66	-129	Dazkırı-Afyonkarahisar	DK

Source: HRV, Harvard CMT Solutions; DK, Kalafat, 2018a, b.

SE / NE-SW direction. This segment is the part of the main fault system which passes near Sultandağı-Çay. Field observations support that an approximately 20 km-break occurred due to this earthquake (Kalafat et al., 2002). Emre et al. found out the following similar results in 2003: the Çay segment is the primary surface faulting caused by the earthquake; it is 20 km long and generally in the east-southwest / west-northwest trending between Maltepe and Pınarkaya villages; Kali Stream segment consists of scattered faults in the northeast-southwest region which runs 6 km long along the edge north of the Kali Stream graben.

The distribution of aftershocks is towards western and northwestern parts of the Sultandağı fault zone and they are generally shallow earthquakes about 10 km depth (Figure 7). The available data support that the energy released as a result of the earthquake move ESE-WNW and NE-SW.

3. Current Data Analysis

The lack of seismic stations in the region and inadequacy of broadband stations in particular have been the most important motivation for the study (Table 3). Though limited, studies were initiated in

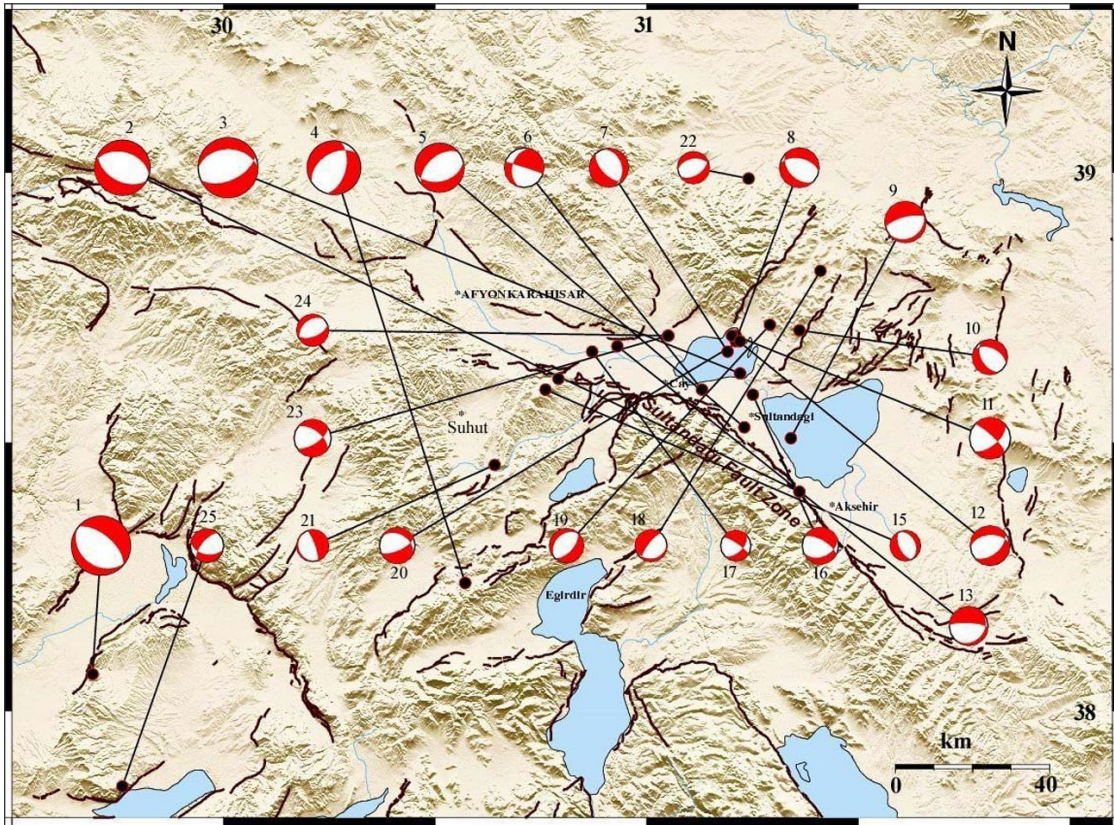


Figure 6- Faulting mechanisms of the earthquakes occurring in the region [of the 25 solutions in the figure, 21 give normal faulting, 4 of them (6, 11, 17 and 23 numbered earthquakes) oblique faulting; active faults were taken from Emre et al., 2013].

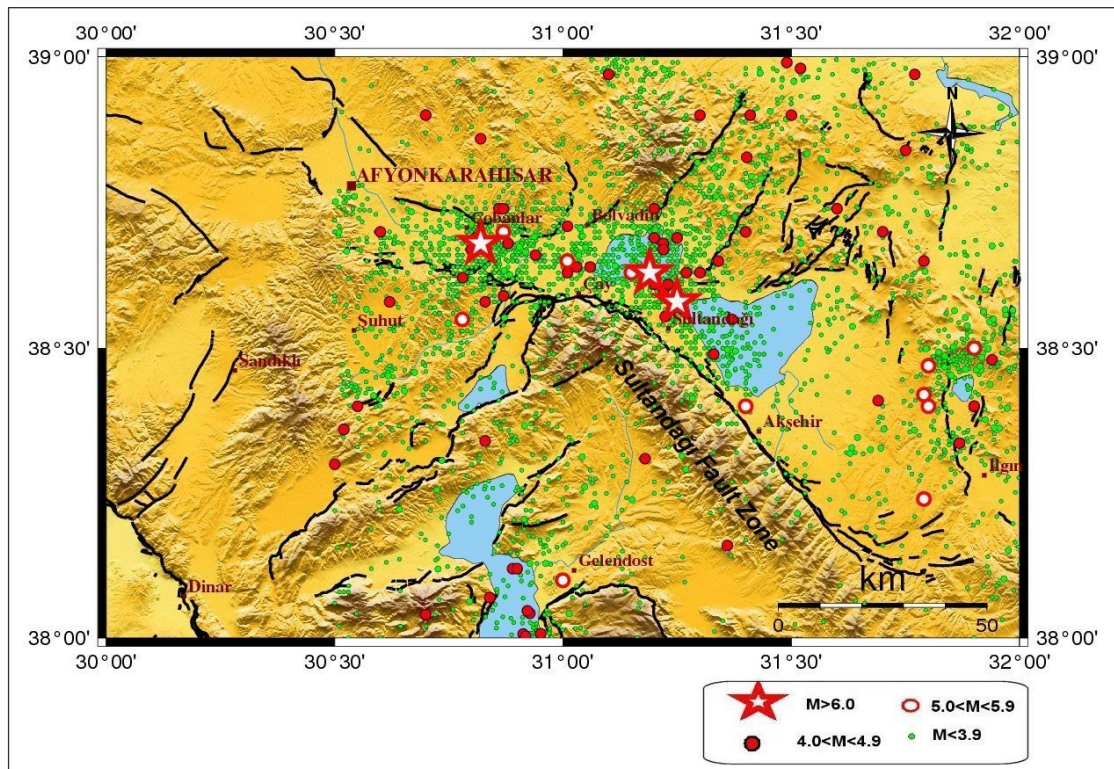


Figure 7- Earthquake activity of the region after the 2000-2002 earthquakes (All of the earthquake focal depths are approximately 10 km. are around and all earthquakes occurred in the shallow depth in the crust; active faults were taken from Emre et al., 2013).

November, 2016. First of all, the locations of 3 new seismic stations were determined. As the 3 major earthquakes ($M_w = 6.0-6.5$) between 2000 and 2002 occurred in the W-NW segment of the Sultandağı fault zone, this particular segment was selected as the location of the stations (Figure 8). While choosing the location, criteria such as safety, ground properties, noise level, logistics were taken into consideration.

Table 3- The stations installed in the region.

Station Name	Station Code	Station Coordinates (deg.)	Sensor Type	Frequency
Koçbeyli	KOCB	38.439513 K - 30.917470 D	Guralp 6-TD	100 Hz
Kırca	KIRC	38.509946 K - 31.232061 D	Guralp 6-TD	100 Hz
Taşagül	TASA	38.794600 K - 31.095050 D	Guralp 6-TD	100 Hz

Data analyses were done in different time periods. The data obtained from each field study were evaluated. The 1st and 2nd Period data sets cover from 18 July 2017 until 27 March 2018. During this period, both the calculations of the data obtained from the stations

installed within the scope of the study and the data obtained from the fixed earthquake station network operated by the Kandilli Observatory and Earthquake Research Institute (KOERI) were compared, and the parameters of the common earthquakes were recalculated. In addition, only the data obtained from the stations which had been installed within the scope of the study were evaluated. When analyzed statistically, the number of 139 events recorded by the KOERI Seismic network during this period (natural earthquakes due to tectonics + unnatural blasting events). The number of 496 events obtained from the stations installed within the scope of the study (Figure 9a, b). The data set obtained in the study is 3.57 times more than the seismic data of KOERI. Therefore, the stations installed within the scope of the study contributed significantly to the seismic monitoring of the region.

Data Set within the Scope of Study: 1st Period of Field Work (17-19 July 2017)

Data Set Date Range: 18 July 2017 (14:23 GMT) - 16 November 2017 (07:13 GMT)

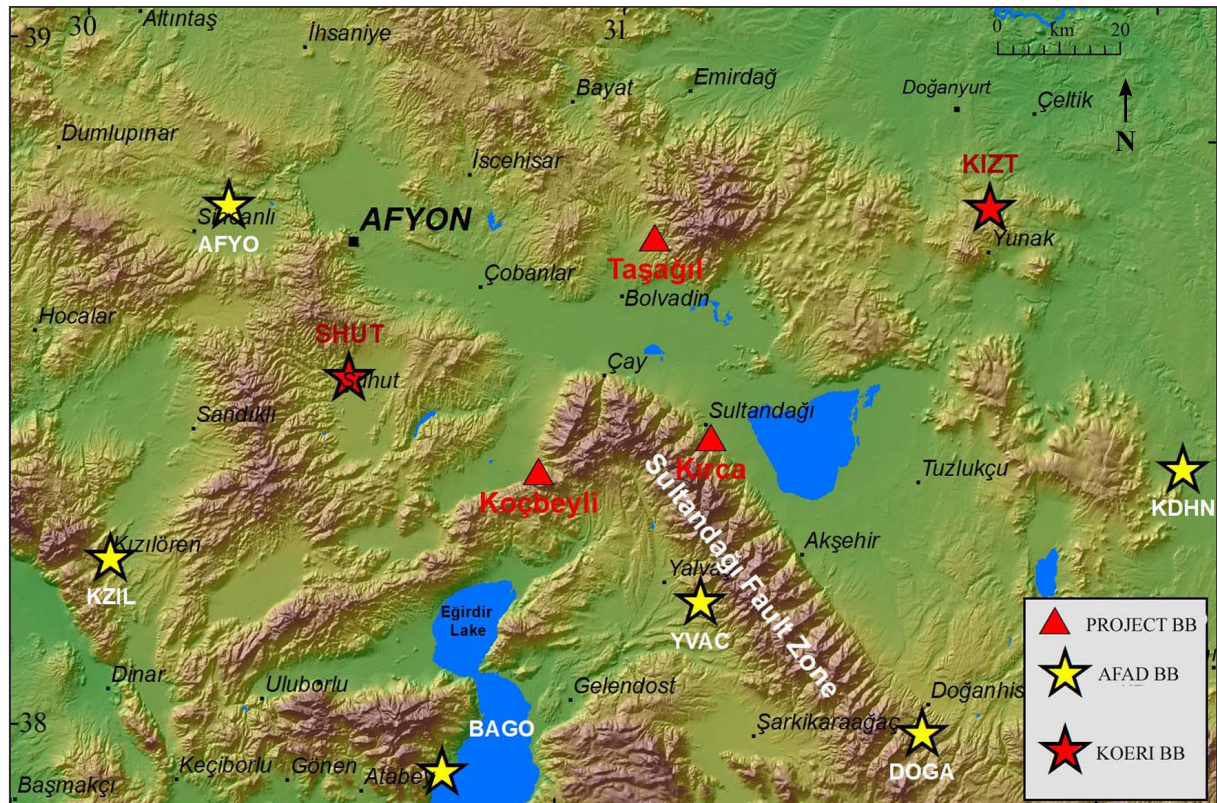


Figure 8- The locations of the stations installed within the scope of the study and operated by KOERI and AFAD in the region.

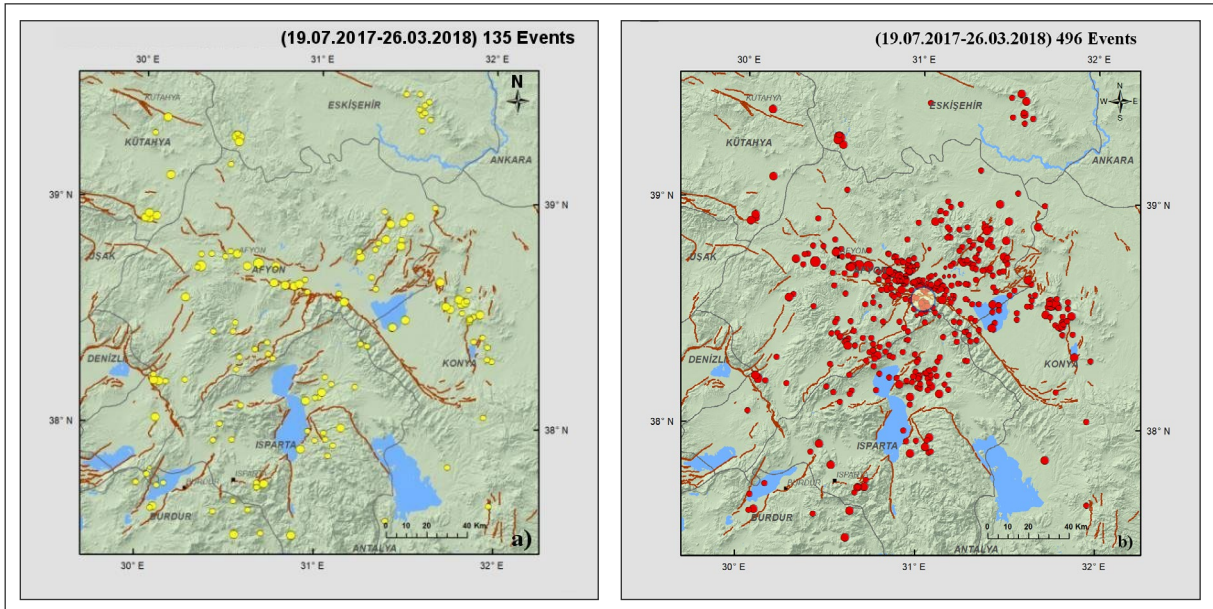


Figure 9- a) Distribution of events recorded by KOERI in the region during the 1st and 2nd periods in which data analysis was conducted (135 events) and b) distribution of events recorded by the stations installed within the scope of the study in the region during the 1st and 2nd periods in which data analysis was conducted (496 events), and light color circle indicates the blast area.

Data Range Coordinates Kandilli Catalog: KOERI
 37.5-39.5 ° N Latitude 30.0-32.0 ° E Longitude

KOERI Total Number of Data: 71 (Earthquake and Blasting)

Data Set within the Scope of Study: 2nd Period of Field Work (25-27 March 2018)

Data Set Date Range: 15 November 2017 (10:15 GMT) - 27 March 2018 (07:00 GMT)

Data Range Coordinates Kandilli Catalog: KOERI
 37.5-39.5 ° N Latitude 30.0-32.0 ° E Longitude

KOERI Total Number of Data: 68 (Earthquake and Blasting)

The stations installed within the scope of the study also contributed very positively to the determination of the epicenters of earthquakes whose solutions were obtained by KOERI. The parameters of the common earthquakes recorded by KOERI and the

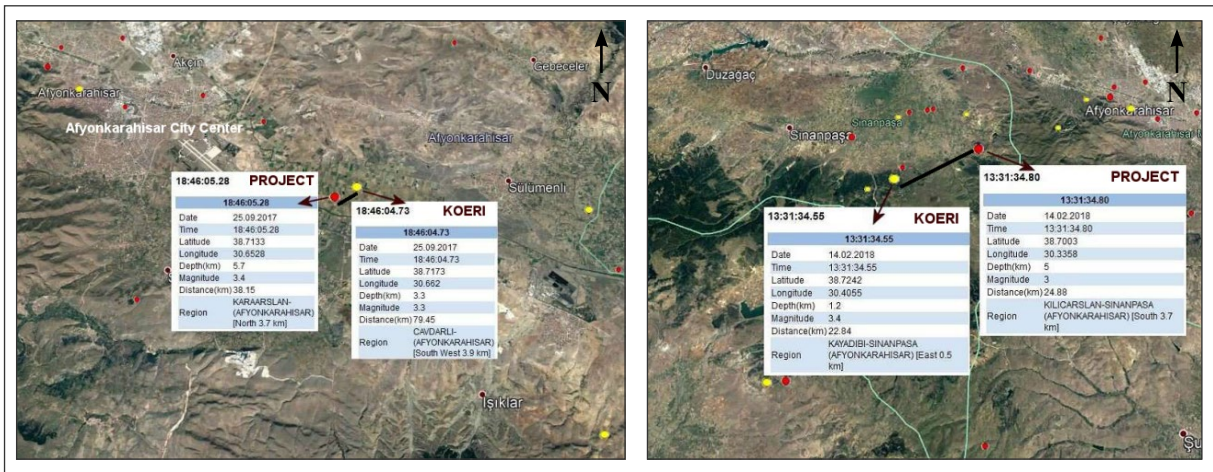


Figure 10- An example which shows how the epicenters of the two different events whose solutions were obtained by KOERI and the stations installed within the scope of the study have changed.

stations installed within the scope of the study were recalculated (Figure 9b). As a result, it was discovered that the epicenters of the earthquakes changed approximately $\pm 0.8-6$ km in average (Figure 10). In addition, the study revealed positive changes in the depth distributions of the earthquakes. As a result, the horizontal and vertical error margins of the events in the region have been reduced thanks to the newly installed stations. The evaluation of the data obtained within the scope of the study indicated that the

middle and northwest part of the Sultandağı-Akşehir fault zone has intense seismic activity. In addition, a significant NW-SE trending seismic activity was determined to the north of Isparta (province).

Figure 11a and 11b shows the distributions and numbers of the earthquakes the data sets obtained by KOERI (a) and within in the study (b) in the same period. It is clearly seen in figure 11a,b that the number of the earthquakes in the data set obtained within the study is much higher.

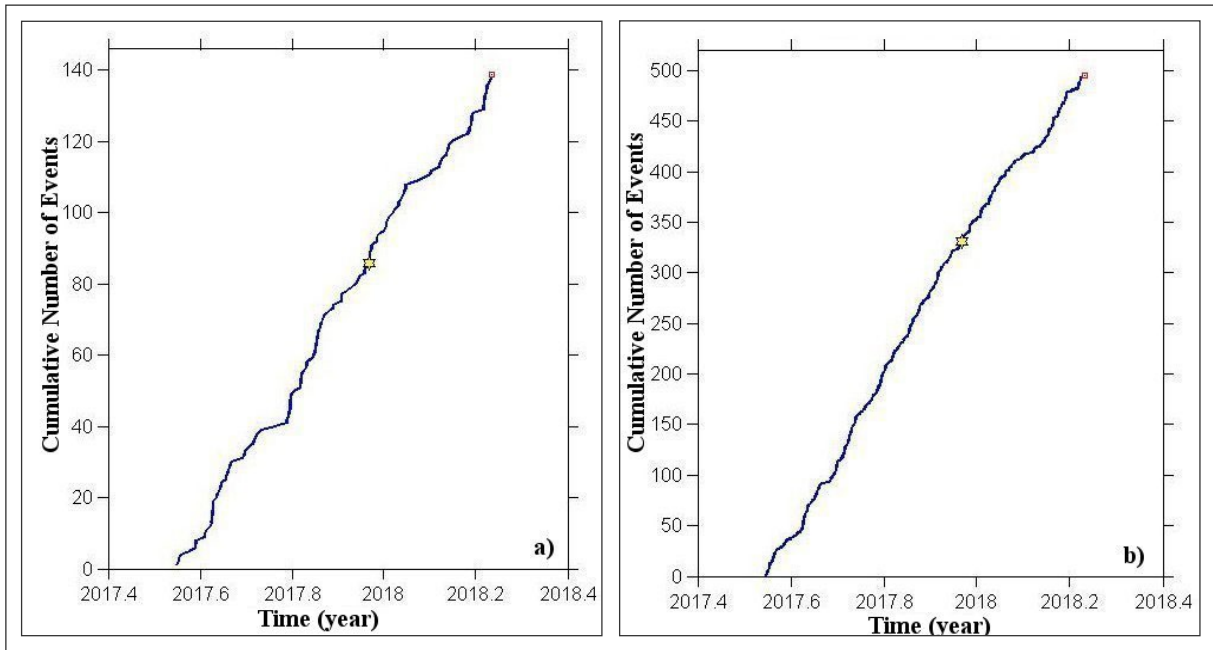


Figure 11- a) KOERI data set b) distribution of the number of the earthquakes in the data set obtained within the study.

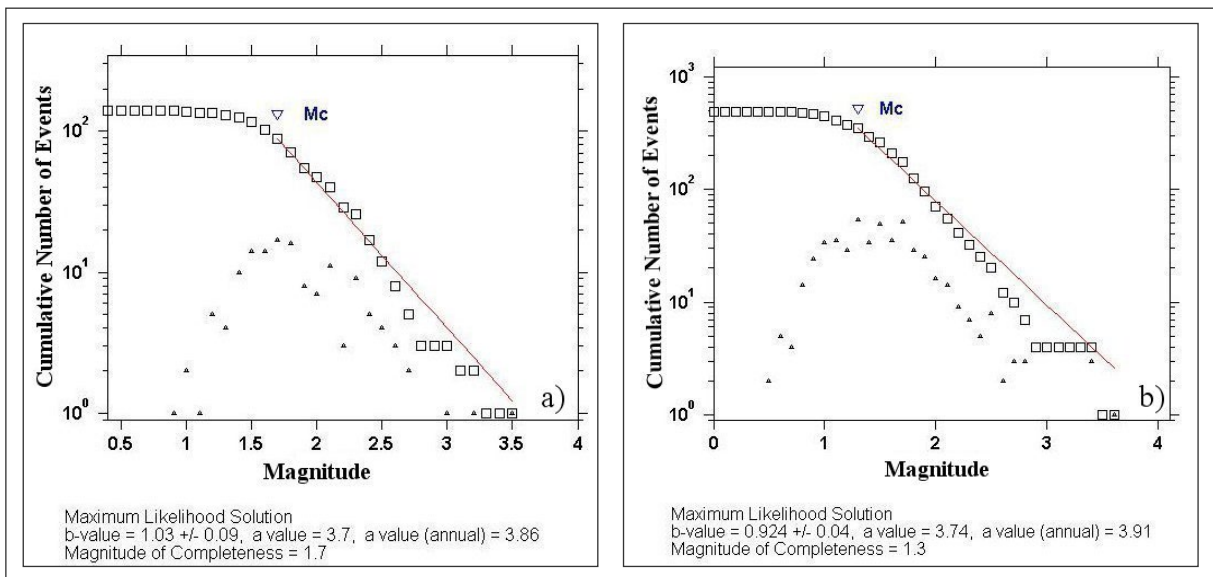


Figure 12- (a) KOERI data set ($M_c = 1.7$), (b) study data set ($M_c = 1.3$).

In the figures below (Figure 12a, b), the lowest magnitude threshold in the KOERI dataset (a) is $M_c = 1.7$; the lowest magnitude threshold in the data set obtained within the study (b) is $M_c = 1.3$. This means that the detection capacity of the fixed seismic network available in the region of KOERI is low ($M_c = 1.7$), and the seismic stations installed within the scope of the study contributed to the increase of the earthquake detection threshold (M_c) sensitivity in the region ($M_c = 1.3$) and increased the detection capacity, revealed that the seismic activity of the region was tracked more precisely.

In the region, especially in some areas, very small events occurring during the day were recorded. During the analysis of the data recorded in the field study, it was concluded that some intense micro-earthquake activity in the study area might have occurred due to the blasts, and therefore some locations where the events took place were detected during the field study. During these visits, we found out that a huge

hydroelectric power plant and, therefore, a dam were being constructed in the area, and that quarry blasts were carried out to supply material in the region. Then, we visited some coordinates present in our records during the data analysis and observed the blasts in these areas (Figure 13).

It was observed that the blasts generally took place at 12:00-13:30/18:00-19:30 LT during the day and this data matches with the seismic records. Therefore, it was also statistically clear that the quarry blasts were carried out at certain time intervals during the day. The magnitude range of the blasts varies between $M = 0.7-2.5$. In the histogram below, the lower part of the red line shows the average number of events that could occur during the day, while the upper part of the red line indicates the number of blasts in the region. Therefore, the hours that display anomalies in the number of earthquakes during the day generally reflect the blasts (Figures 14, 15).



Figure 13 - Blast locations conducted for the embankment of Çay Dam.

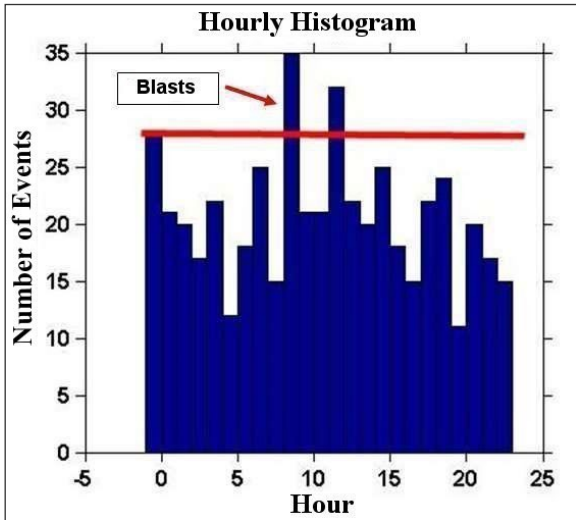


Figure 14- Hourly change of the events and blasts in the region during the day (GMT).

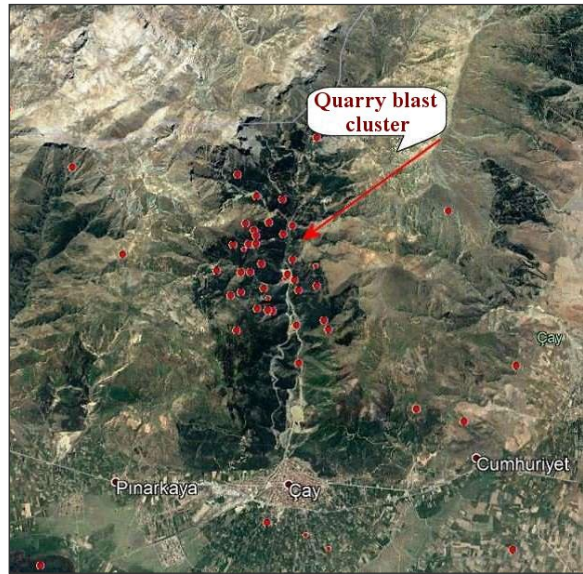


Figure 15- Blasting cluster analyzed within the scope of the study (south of Çay district, dam construction area).

The third data set analysis covers the period between 20 March 2018 and 15 March 2019. During this period, both the calculations of the data obtained from the stations installed within the scope of the study and the data obtained from the fixed earthquake station network operated by KOERI were compared, and earthquake parameters (coordinates, depth, magnitude, RMS root mean square residual, ERH horizontal error, and ERZ vertical error) of the common earthquakes were recalculated. This study evaluated only the data

obtained from the stations which had been installed within the scope of the study. The statistics show that the number of events recorded by the KOERI seismic network during this period (natural earthquakes due to tectonics + unnatural blasting events) is 341. The number of events detected in the study is 480 (Figure 16a, b). In short, the data obtained within the scope of the study was approximately 41% higher than the seismic data of KOERI. Therefore, the stations

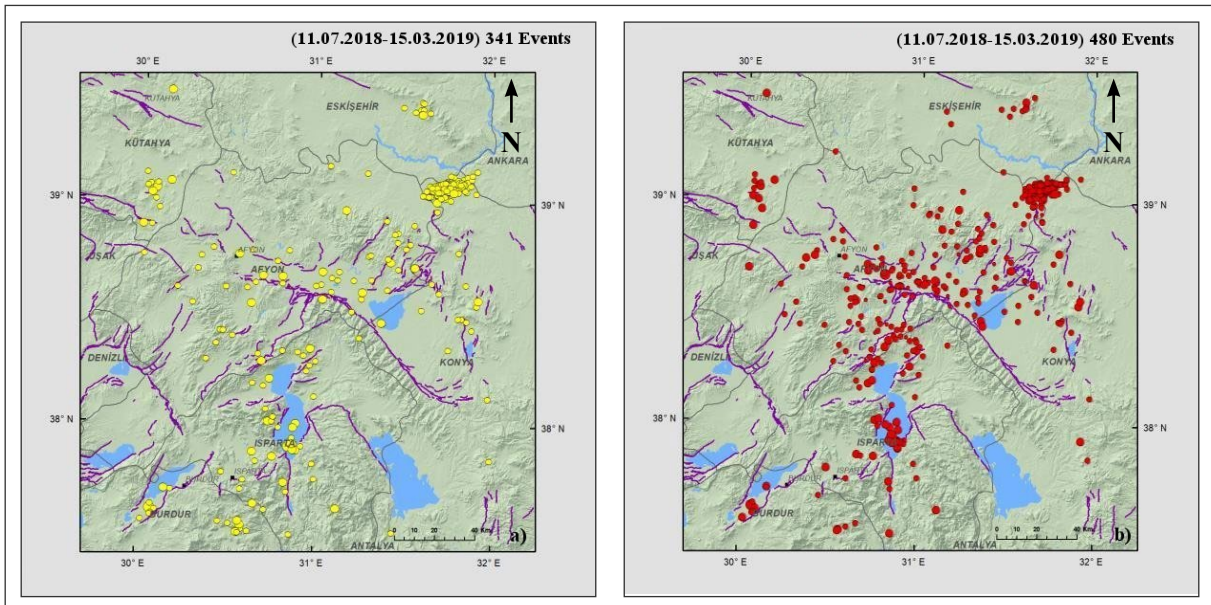


Figure 16 - a) Distribution of events recorded by KOERI in the region during the 3rd period in which data analysis was conducted (341 events). b) Distribution of events recorded in the scope of the study in the 3rd period (480 events).

installed within the scope of the study have made a great contribution to the seismic monitoring of the region and to the seismotectonics.

It was observed that the earthquake epicenters that were recalculated changed approximately ± 0.5 -2.6 km on average (Figure 17). In addition, the study revealed some positive changes in the depth distributions of the earthquakes. As a result, the horizontal and vertical error margins of the events in the region were reduced thanks to the newly installed stations. As a result of the evaluation of all data, it was observed that especially the NE of Doğanyurt, the vicinity of Eğirdir Lake, Altıntaş-Kütahya, Çobanlar-Bolvadin-Çay, especially the middle and northwestern part of the Sultandağı-Akşehir Fault Zone have intense seismic activity.

Figure 17 is given as an example of how the epicenters of three different events changed with the new data obtained in the study. In the 3rd period, it was observed that there were no intense quarry blasts in the region. Local micro-earthquake activities, blasts and tele-seismic (distance earthquake) records were monitored in the 3rd period data set evaluated within the scope of the study.

4. Related Theories and Methods Used

Different software and techniques were used in this study. The most important of them were the software that are still widely used by the world's major seismology centers for the calculation of earthquake parameters (Hypo71, HypoInv, Hypocenter; Lee and

Lahr, 1975; Klein, 1985; Lienert et al., 1986). Station distribution and density are of great importance in determining the locations of earthquakes. Earthquake locations can be calculated very accurately with a well-designed station distribution considering the intended target. The stations installed within the scope of the study were designed for these purposes. Three component digital data obtained from the stations were used in the Hypocenter program used within the scope of the study. All prepared data which were entered into the program as an input file, so all parameters such as occurrence time, geographic coordinates, size and depth of earthquakes were determined by inverse solution algorithm. The program attempted to determine the location of the earthquake in a way that can minimize the difference between the theoretical P- and S-arrival times created according to a given ground seismic velocity structure (Kalafat et al., 1987) and the observational times read from the data.

Another method targeted and used within the scope of the study was to enable the magnitude of earthquakes to be given by different methods. In this study, M_L Local magnitude was given to all earthquakes in general, and M_w Moment magnitude calculation was made for earthquakes with $M > 3.3$ in general. Richter (1936, 1948) magnitude, also defined as Local magnitude (M_L), is the magnitude type used by all seismology centers in local earthquake studies. The definition of the method was made according to the Wood-Anderson (WA) seismometer used at that time. In this study, the calculation method determined by KOERI was used. The earthquake records obtained

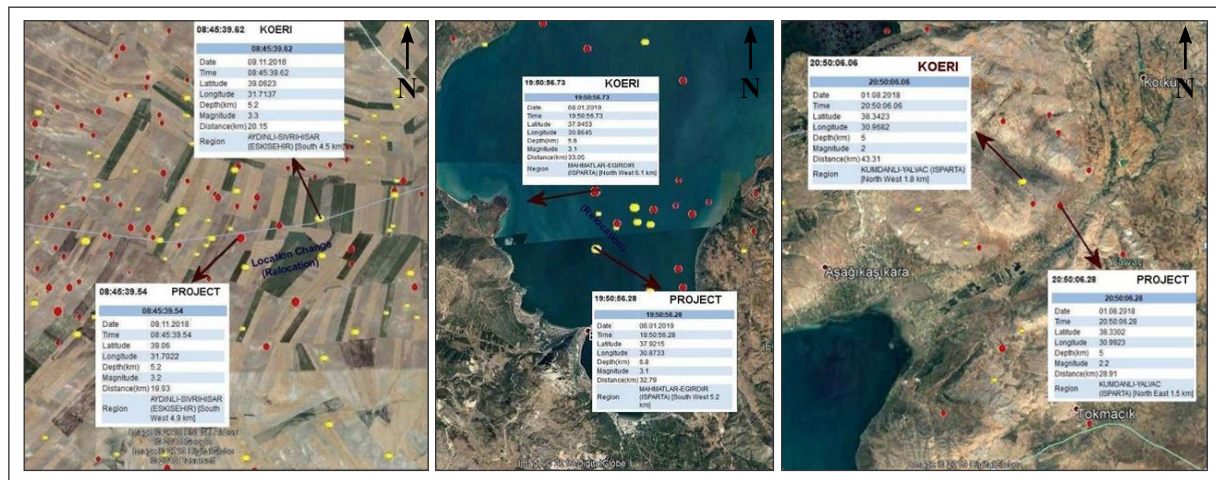


Figure 17- Examples showing both the new solutions of three earthquakes aside from the changes in their locations thanks to the stations installed within the scope of the study and the solutions obtained from KOERI.

within the scope of the project were converted into WA record with signal analysis methods and used in accordance with this definition. Briefly, they were simulated to the original WA seismometer. In the Richter approach, the basic expression is the ratio of the maximum amplitude (A) observed at the station to the reference amplitude (A₀):

$$M_L = \log \frac{A}{A_0}$$

A is the maximum (in mm) zero-to-peak amplitude (+ or -) recorded by a WA seismograph. A₀ is the amplitude of the zero magnitude earthquake as a function of the epicentral distance. Moment magnitude (M_w) was generally given as a result of the determination of earthquake source parameters or by using S wave spectrum technique. Below are the Moment Magnitudes (M_w) given by the BLVD and SDAG stations used within the scope of the study

and their contribution to the solution of the Darıcılar-Dazkırı (Afyonkarahisar) earthquake on 8 August 2019 (Figure 18).

In addition, these stations also contributed to the determination of the Earthquake Source Parameters, and the digital data obtained enabled the calculation of fault plane solutions of earthquakes with a magnitude M > 3.5. Relevant programs were used for the analysis of the data obtained from the digital three-component records collected in the study (Dreger 2002; Sokos and Zahradník, 2013; Figure 19).

Within the scope of the study, Earthquake Source Parameters of the Acıpayam earthquakes that occurred in the region in 2019 were calculated through the Moment Tensor Inversion (MTI) technique (Figure 20; Table 3). In addition, regional stress analysis was performed using the stress analysis method (Gephard, 1990). In the stress analysis of 15 earthquakes using P

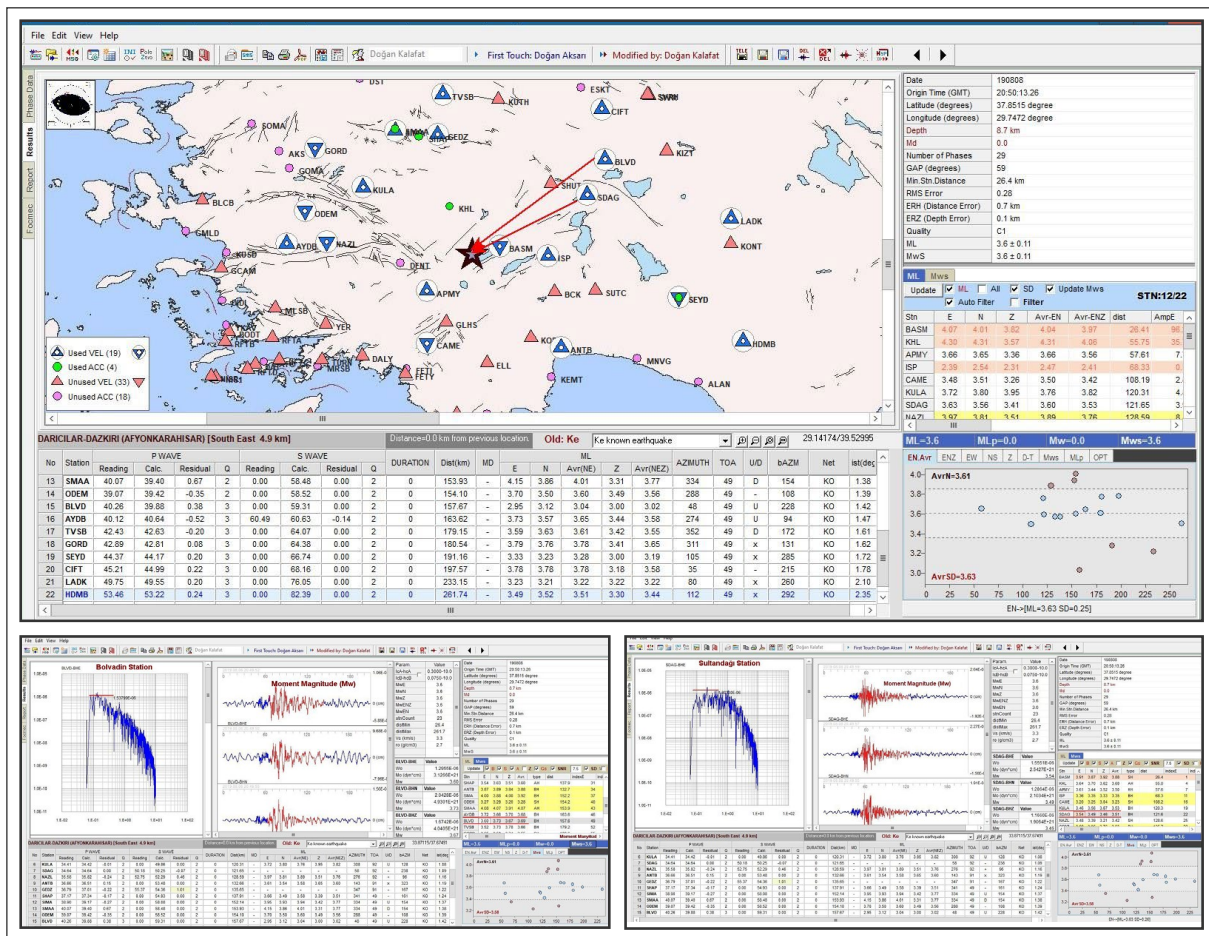


Figure 18- The contribution of the Bolvadin (BLVD) and Sultandağı (SDAG) stations to the solution of Darıcılar-Dazkırı (Afyonkarahisar) earthquake on 8 August 2019.

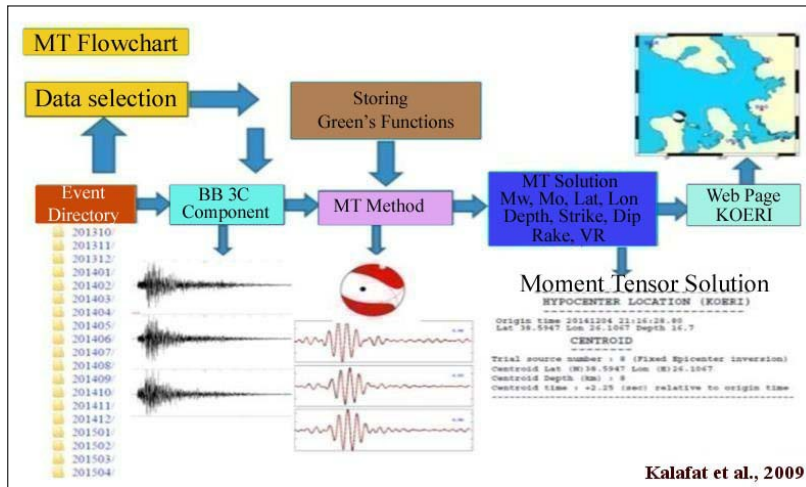


Figure 19 - Fault plane/MT solution flowchart (Kalafat et al., 2009; Kalafat, 2016).

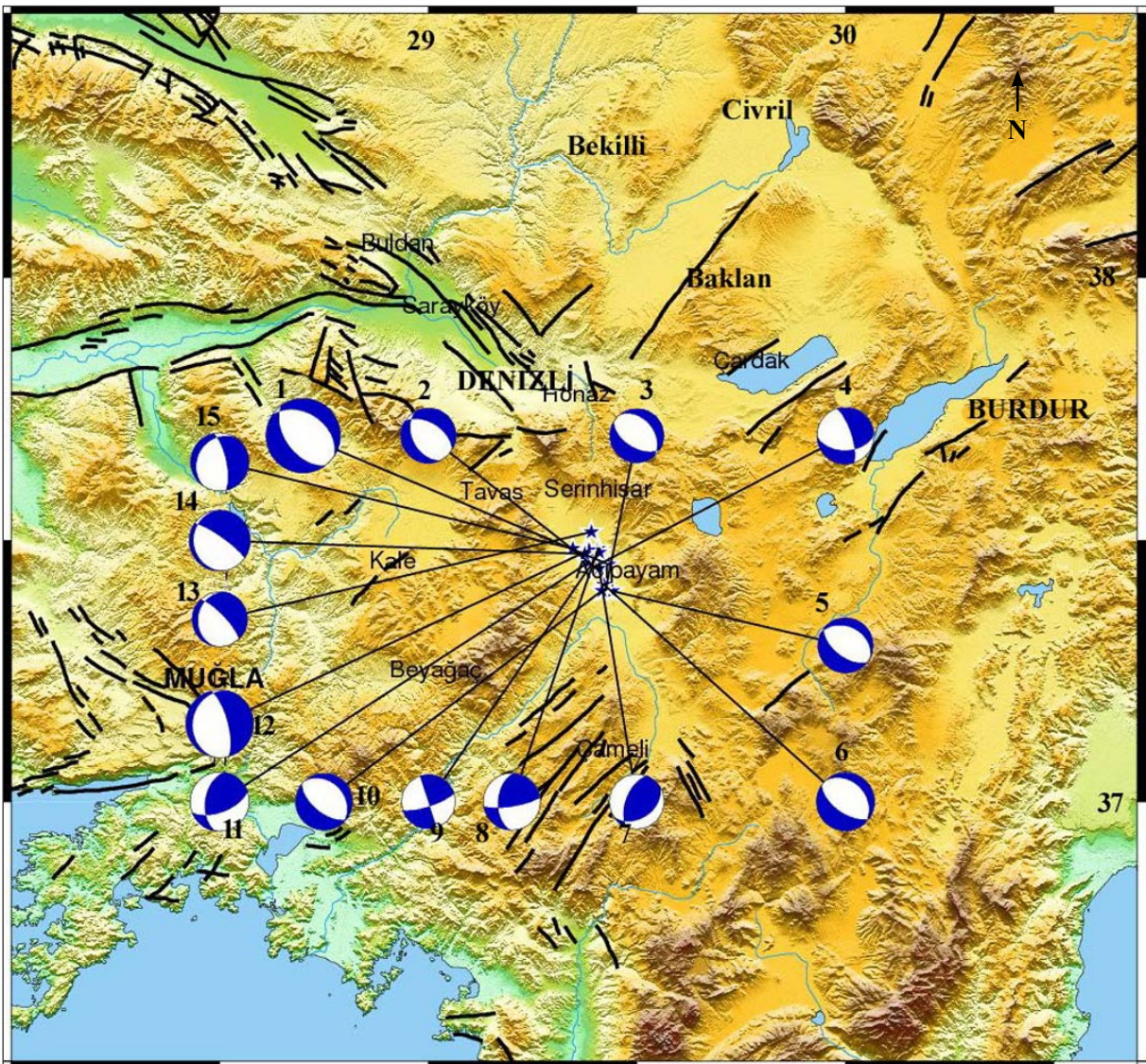


Figure 20 - Fault plane solutions of Denizli-Acıpayam earthquakes that occurred in the region in 2019.

Table 3- Fault Plane Solutions of the 2019 Acipayam-Denizli earthquakes.

EQ. No.	Date	Time	Lat.	Lon.	Depth.	Mw	Str.	Dip A.	Rake A.
					km.				
1	20.03.2019	06:34	37.4545	29.4317	12	5.5	304	40	-105
2	20.03.2019	06:51	37.446	29.405	6	4.1	302	52	-110
3	20.03.2019	08:00	37.4075	29.4252	6	4	121	54	-102
4	20.03.2019	12:45	37.4523	29.4025	6	4.2	89	47	-156
5	20.03.2019	17:04	37.4035	29.441	8	4.1	296	33	-100
6	20.03.2019	17:42	37.4163	29.421	8	4.3	317	31	-80
7	22.03.2019	08:20	37.4475	29.4098	20	4.1	201	57	68
8	22.03.2019	15:32	37.4845	29.4075	14	4.2	183	50	18
9	24.03.2019	16:17	37.4777	29.4105	8	4	72	76	-180
10	25.03.2019	06:15	37.4047	29.4163	8	4.2	129	60	-94
11	27.03.2019	11:27	37.4592	29.3848	15	4.4	188	49	40
12	31.03.2019	11:30	37.4815	29.385	8	5	345	71	-99
13	31.03.2019	11:45	37.5167	29.3905	8	4.1	316	76	-108
14	01.04.2019	01:49	37.4747	29.3745	8	4.5	305	80	-101
15	04.04.2019	15:01	37.4848	29.3468	8	4.3	348	72	-107

and T axes (azimuth – plunge), the general direction of the main axes is E-W (P) trending compression and N-S (T) trending extension.

In general, stress tensors are obtained by using fault plane solutions. These are the directions of the three principal stress axes (Sigma1 > Sigma2 > Sigma3) and the relative quantities explained by the Stress ratio (R) for the principal stress axes. The stress regime is expressed according to which of them is in the vertical plane. When the greatest principal stress

axis (Sigma1) is vertical, this indicates extensional tectonics; when the intermediate principal stress axis (Sigma 2) is vertical, this indicates strike-slip tectonics; and when the minimum principal stress axis (Sigma 3) is vertical, this indicates compressional tectonics.

The fact that the dips of the principal stress axes Sigma 1 and Sigma 3 are close to horizontal and the dips of Sigma 2 are close to vertical indicates a dominant Strike-slip Faulting regime. The solution

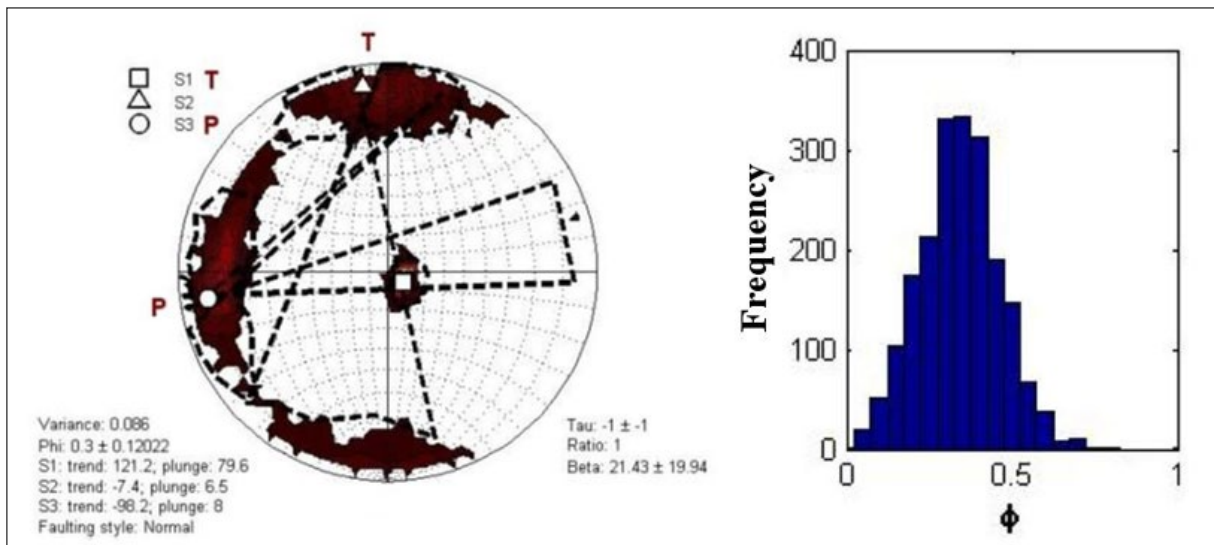


Figure 21 - Stress analysis performed in the study (The dominant directions of the principal stresses, the value of the R stress ratio).

from the study is the opposite and shows that the vertical slip normal faulting regime is dominant in the region (Figure 21).

$\text{Sigma}_2 - \text{Sigma}_1 / \text{Sigma}_3 - \text{Sigma}_1 = R$ shows the amplitude values of the principal stress axes in the region. R_{max} = stress ratio R shows the relationship between the 3 principal stress axes. The fact that $0 \leq R \leq 1$ and $R(\phi)$ is between 0-0.5 indicates that an extensional tectonic regime is dominant in the region, and that this extensional regime continues its current evolution with vertical slip normal faults.

5. Results and Discussion

The study showed that the stations installed within the scope of the study decreased the earthquake detection threshold (M_c) in the region to $M_c = 1.3$

(Figure 22). This made a significant contribution to the monitoring of micro-earthquake activity very sensitively especially in the Sultandağı Fault Zone (SFZ) and its surrounding. It has been observed that as the sensitivity of the seismic network increases and the detection threshold (M_c) decreases, the number of earthquakes detected from the region increases significantly. The number of earthquakes that occurred in the region only during the study period is 1442 (Figure 23).

All Data Set in the Study Period (Between 19.07.2017 and 11.07.2019); while the number of Total KOERI Solutions is 638, the number of total solutions within the study is 1442 (Table 4; Figure 23; 24a, b). The comparison of the data obtained by KOERI and the study is below.

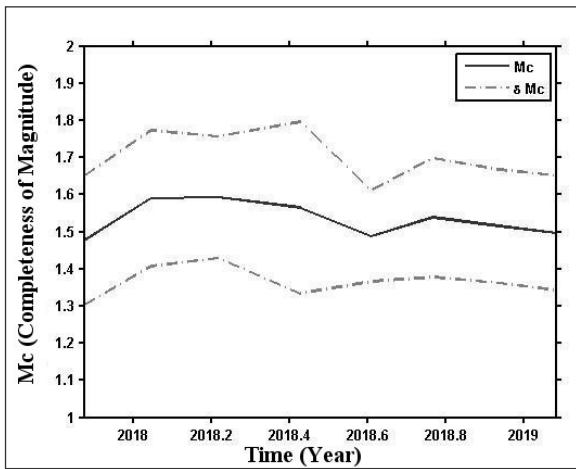


Figure 22- M_c range of earthquake detection threshold within the project.

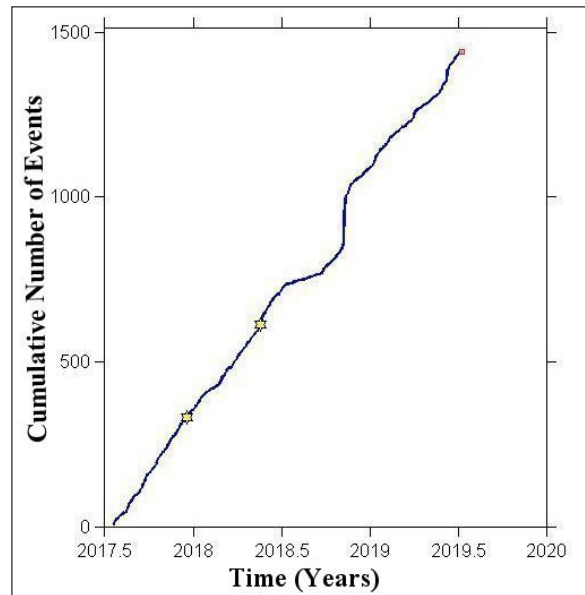


Figure 23- The cumulative increase in the number of events evaluated within the study.

Table 4- Comparison of data obtained by KOERI and the study.

PERIOD	DATE RANGE	KOERI SOLUTIONS	WITHIN THE STUDY	INCREASE
			AFTER EVALUATION	
		Number of Events	Number of Events	Number of Events
1-2.	19.07.2017-26.03.2018	135	496	361
3	27.03.2018-10.07.2018	79	236	157
	11.07.2018-14.03.2019	341	481	140
	15.03.2019-11.07.2019	83	229	146
TOTAL		638	1442	804

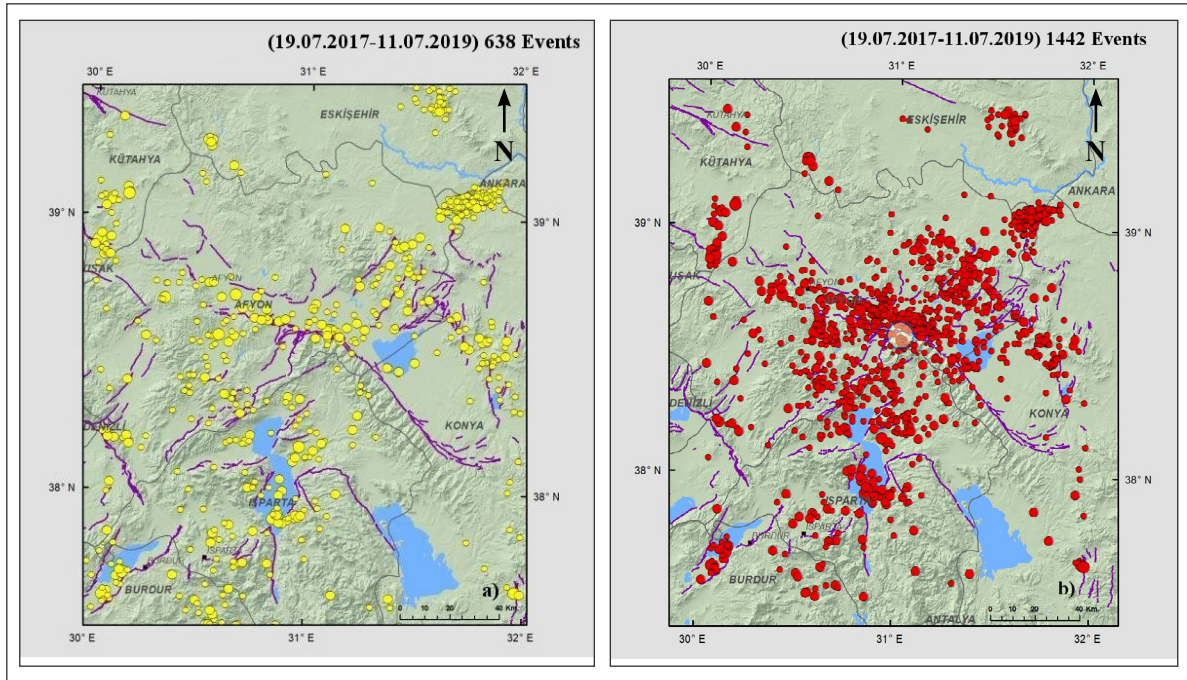


Figure 24- a) KOERI Solutions during the study period and b) solutions obtained with the contribution of the stations installed within the scope of the study (Active faults are from Emre et al., 2013; topography data is from NASA-SRTM).

In short, the number of earthquakes in the region whose parameters were calculated increased 2.26 times during the study. This has made a significant contribution to eliminating the lack of data in earthquake catalogs, monitoring the pre-earthquake process of earthquake generating sources, revealing the earthquake occurrence patterns, monitoring the energy discharge of the region, and calculating the cumulative seismic moment (Figure 25).

During the study, we recorded quarry blasts during the day conducted to supply material for

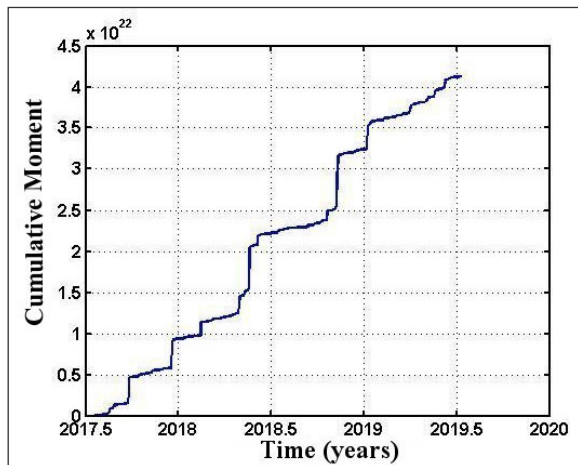


Figure 25 - Cumulative moment increase in the scope of the study.

the construction of the dam in the region. Thus, the sensitivity of the unnatural events catalog data set was increased by entering the coordinates of the blast areas into the existing database in the earthquake analysis of KOERI regarding the detection of the blast areas throughout the country (Figure 26a, b).

As a result of the study, it was observed that the central and western parts of the SFZ are active, and that especially the vicinity of Sultandağı, Çay, Çobanlar and Afyonkarahisar have intense seismic activity. It was observed that there was a cluster of events owing to blasts during the construction of the Çay Dam to the south of Çay district. In addition, intensive seismic activities were observed along the south-southeast of Eğirdir Lake and to the south of Burdur Lake (Figure 24b).

The greatest contribution of the study is that two of the stations installed within the project were integrated into the National Seismic Network of Turkey operated by KOERI after the project was completed, enabling the existing network to serve more precisely across the country (Figure 27, 28).

The data obtained by the two stations installed within the scope of the study flow to RETMC

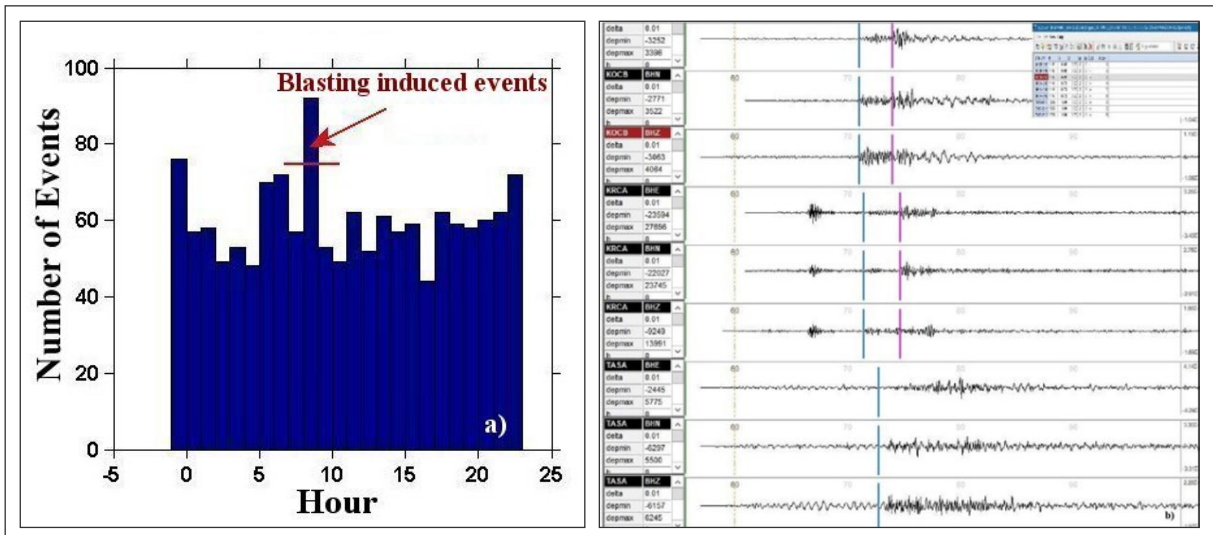


Figure 26- Unnatural blast event in the study area a) the distribution during the day and b) example of blast waveforms recorded by the installed stations (14.04.2018 15:11 GMT Çay-Afyon $M = 0.9$).

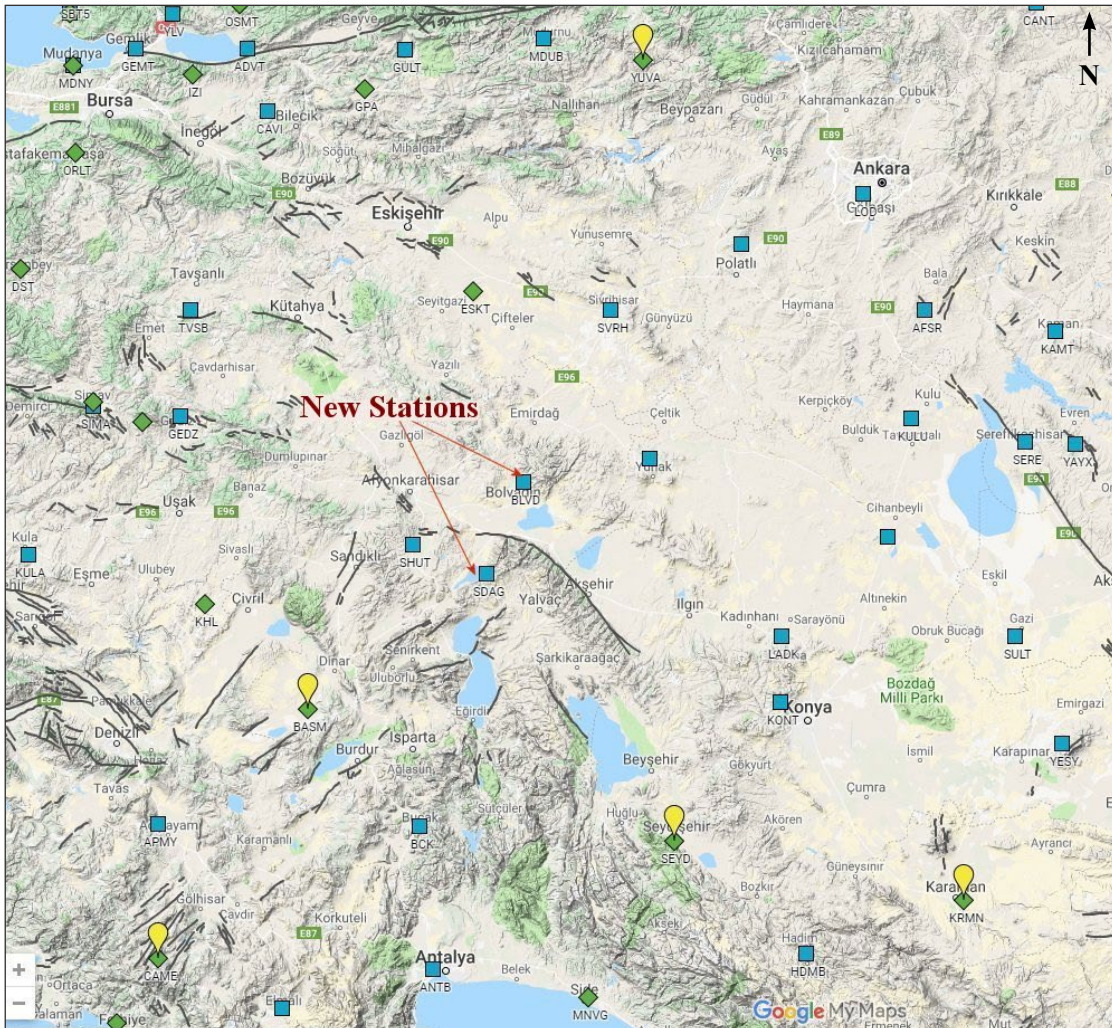


Figure 27- Two project stations, which are KOCB Koçbeyli and TASA Taşağıl, are integrated into National Seismic Network of Turkey. These stations are registered by ISC as BLVD and SDAG.

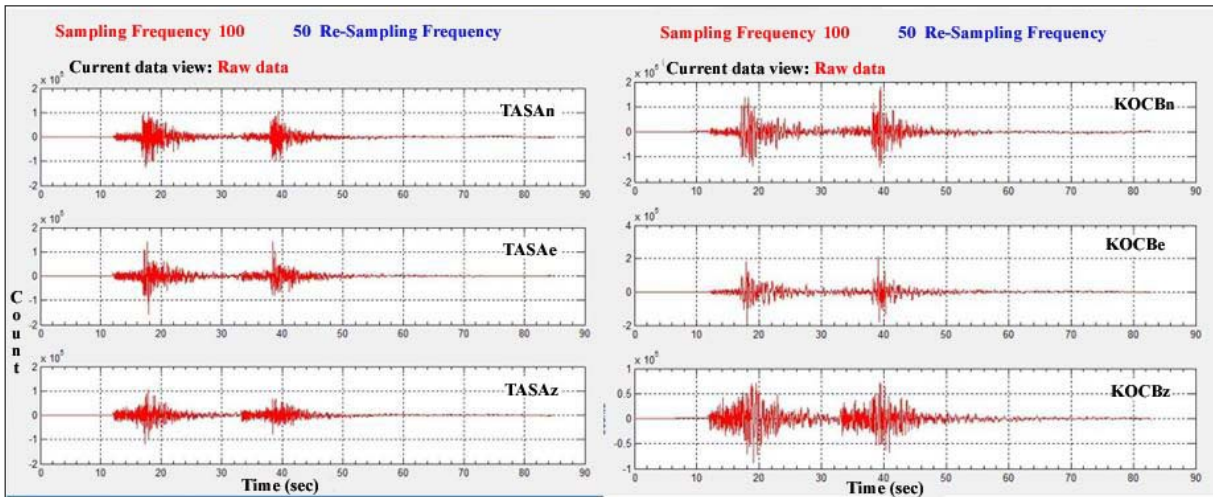


Figure 28- An example of sequential earthquakes recorded by the stations installed.

(Regional Earthquake-Tsunami Monitoring Center) in real-time. The stations installed were registered with the International Seismology Center (ISC); their International Station Codes were assigned (SDAG and BLVD) and they were included in the Global Seismic Network List. These stations contributed greatly to the solutions of the earthquakes that occurred in Western Anatolia recently. The 8 August 2019 Denizli Earthquakes can pose the best example for this. In the examples below (Figure 29), the contributions of these stations installed within the scope of the study to the Denizli Earthquake activity can be seen.

It was found that the locations of the earthquakes which were relocated by the installed stations changed with an average of ± 0.5 -2.6 km. In addition, the study revealed positive changes in the depth distributions of the earthquakes. As a result, the horizontal and vertical error margins of the events in the region reduced thanks to the stations installed, and these stations greatly contributed to the development of the existing

seismic network sensitivity. Therefore, the stations installed will have a remarkable contribution to find the answer to the questions whether the earthquake activity that might occur in the period after the three major earthquakes in the region in 2000 and 2002 will continue towards the NW or in a different direction. In this context, seismic monitoring in SFZ is crucial and it should not be ignored that the active fault segments to the west of Çay and northwest of Çobanlar carry a high seismic risk in the future.

Acknowledgements

This study was supported by Boğaziçi University under BAP Project No: 12280. Hereby, we would like to express our thanks to the Boğaziçi University Research Fund Commission and its valuable members. The authors would also like to thank Dr. Selim Özalp (the referee), Dr. Asuman Kahya (the technical editor), Assoc. Prof. Dr. Şule Gürboğa (the assistant editor), Dr. Narumi Takahashi and the anonymous referee for their constructive contributions and critiques they provided throughout the examination of the article.

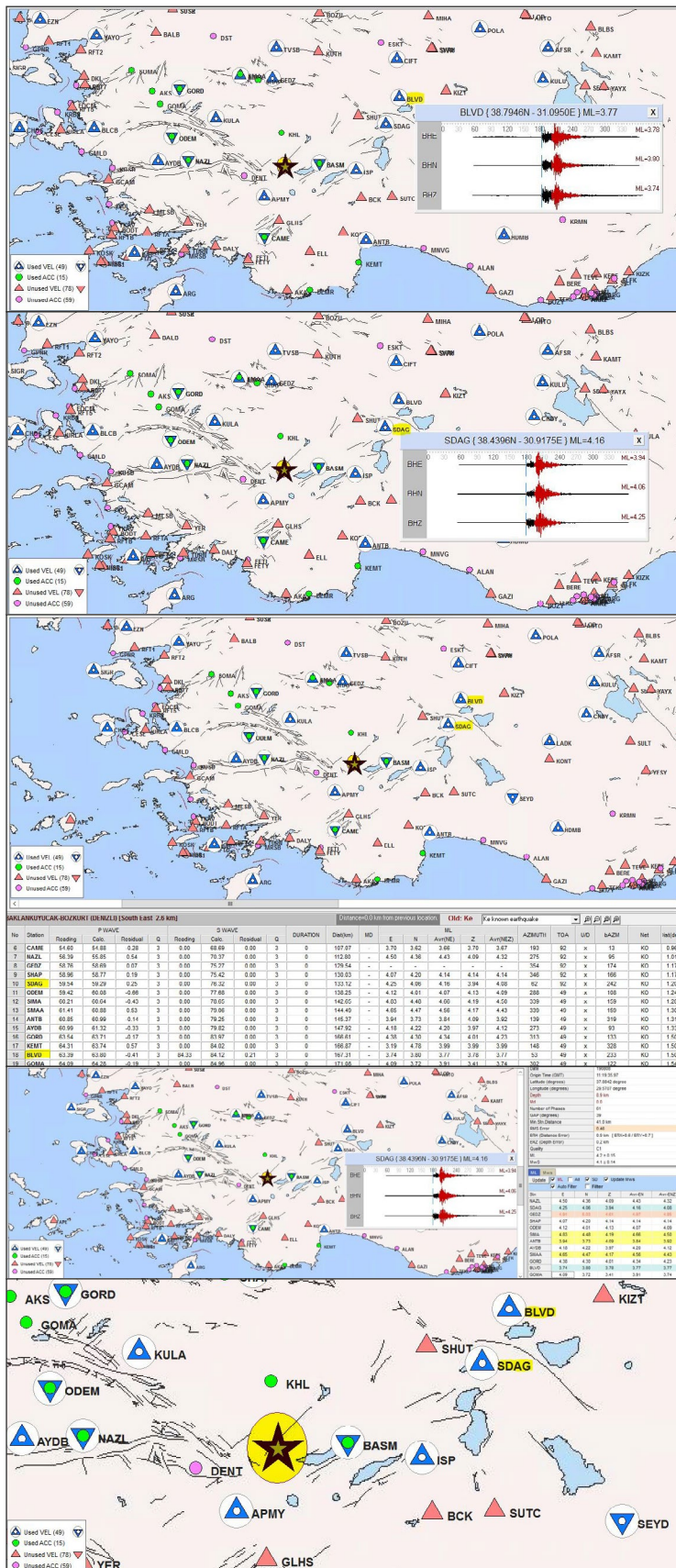


Figure 29- Contribution of Sultandağı (SDAG) and Bolvadin (BLVD) stations to the solutions of the 8 August 2019 (11:19 and 20:50 GMT) Denizli earthquakes.

References

- Akyüz, S., Uçarkuş, G., Şatır, D., Dikbaş, A., Kozacı, Ö., 2006. 3 Şubat 2002 Çay depreminde meydana gelen yüzey kırığı üzerinde paleosismolojik araştırmalar. *Yerbilimleri*, 27 (1), 41-52.
- Altunel, E., Barka, A., Akyüz, S. 1999. Palaeoseismicity of the Dinar fault, SW Turkey. *Terra Nova*- 11, 297-302.
- Atalay, I. 1975. Tektonik hareketlerin Sultandağları'nın jeomorfolojisine olan etkileri, *Türkiye Jeoloji Kurumu Bülteni* 18, 21-26.
- Barka, A.A., Reilinger, R.E., Şaroğlu, F., Şengör, A.M.C. 1995. Isparta Angle: its importance in the neotectonics of the Eastern Mediterranean Region. In: Pişkin, D., Ergün, M., Savaşın, M.Y. and Tarcan, G. (eds), *International Earth Science Colloquium on the Aegean Region Proceedings*-3-18.
- Blumenthal, M. M. 1963. Le systeme structural du Taurus sud Anatolien, *Paul Fellot*, 2, Societe Geologique de France, 611-662.
- Boray, A., Şaroğlu, F., Emre, Ö. 1985. Isparta bölümünün kuzey kesiminde doğu-batı daralma için veriler. *Jeoloji Mühendisliği Dergisi* 23, 9-20.
- Dreger, D. 2002. Time-Domain Moment Tensor INverse Code (TDMT_INV) Version 1.1, Berkeley Seismological Laboratory, 18.
- Emre, Ö., Duman, T. Y., Doğan, A., Özalp, S., Tokay, F., Kuşçu, İ. 2002. 3 Şubat 2002 Sultandağı Depremi Ön Değerlendirme Raporu (Mw=6.3), Maden Tetkik ve Arama Genel Müdürlüğü, (<http://www.mta.gov.tr/v3.0/bilgi-merkezi/afyon>).
- Emre, Ö., Duman, T. Y., Doğan, A., Özalp, S., Tokay, F., Kuşçu, İ. 2003. Surface Faulting Associated with the Sultandağı Earthquake (Mw 6.5) of 3 February 2002, Southwestern Turkey, *Seismological Research Letters* 74, 4, 382-392.
- Emre, Ö., Duman, T. Y., Özalp, S., Elmacı H., Olgun, Ş., Şaroğlu, F. 2013. Açıklamalı Türkiye Diri Fay Haritası. Ölçek 1:1.250.000, Maden Tetkik Arama Genel Müdürlüğü, Özel Yayın Serisi-30, Ankara.
- Eyidoğan, H., Güçlü, U., Utku, Z., Değirmenci, E. 1991. Türkiye Büyük Depremleri Makro-Sismik Rehberi (1900-1988), İTÜ MF Jeofizik Mühendisliği Bölümü Yayınları s. 200.
- Gephard, J.W. 1990. FMSI: A FORTRAN program for inverting fault/slickenside and earthquake focal mechanism data to obtain the original stress tensor. *Comput Geosci* 16, 953-989.
- Glover, C., Robertson, A. 1998. Neotectonic intersection of the Aegean and Cyprus tectonic arcs: extensional and strike-slip faulting in the Isparta Angle, SW Turkey. *Tectonophysics* 298, 103-132.
- GMT v4 The Generic Mapping Tools, <http://gmt.soest.hawaii.edu/gmt4/>.
- HRV Harvard Centroid-Moment Tensor Project CMT, Harvard University, MA, USA (1977-2017) <https://www.globalcmt.org/>.
- Kalafat, D. 1996. 1 Ekim 1995 Dinar Depremi ve Saha Gözlemleri. *Deprem Araştırma Bülteni* 74, 95-113.
- Kalafat, D. 2016. Türkiye ve Çevresi Faylanma-Kaynak Parametreleri (MT) Kataloğu (1938-2015) / A Catalogue of Source Parameters of Moderate and Strong Earthquakes for Turkey and its Surrounding Area (1938-2015), Tubitak Technical Report, 2016.
- Kalafat, D. 2018a. Türkiye ve Çevresi Moment Tensör-Faylanma Bilgi Bankasının Oluşturulması ve Bölgesel Gerilme Analizleri, Türkiye Ulusal Jeodezi Jeofizik Birliği Bilimsel Kongresi – Scientific Congress of the Turkish National Union of Geodesy and Geophysics, Bildiri Kitabı-Abstract Book p. 462-469, 30 Mayıs-02 Haziran 2018, İzmir-Turkey.
- Kalafat, D. 2018b. Source Parameters of Moderate and Strong Earthquakes for Turkey and its Surrounding Area (1938- 2017), JpGU Meeting 2018 Japan Geoscience Union, Presentation Number: S-SS08, 20-24 Mayıs 2018 Makuhari Messe Chiba, Japan.
- Kalafat, D., Öz, G. 2001. 15 Aralık 2000 Sultandağı-Bolvadin (Afyon) Depremi, Türkiye 14. Jeofizik Kurultayı ve Sergisi, Genişletilmiş Sunu Özetleri Kitabı (Extended Abstracts Book) 26-31, MTA Kültür Merkezi, 8-11 Ekim 2001, Ankara (in Turkish).
- Kalafat, D., Görgün, E. 2017. An example of triggered earthquakes in western Turkey: 2000–2015 Afyon-Akşehir Graben earthquake sequences, *Journal of Asian Earth Sciences* 146 (2017) p.103-113.
- Kalafat, D., Gürbüz, C., Üçer, S.B. 1987. Batı Türkiye' de Kabuk ve Üst Manto Yapısının Araştırılması, *Deprem Araştırma Bülteni* 59, 43-64 (in Turkish).
- Kalafat, D., Öz, G., Kara, M., Ögütçü, Z., Kılıç, K., Pınar, A., Yılmaz, M. 2000. 1981-1997 Türkiye ve Dolayları Deprem Kataloğu (M>4.0), B.Ü. Yayınları 2000, Bebek, İstanbul.
- Kalafat, D., Kuleli, S., Li, X., Toksöz, M. N., Gulen, L. 2002. The Afyon Turkey Earthquake: Source Characteristics and Implications for Earthquake Triggering, Eastern Section of the Seismological Society of America, Program and Abstracts p.16,

- 74th Annual Meeting October 20-22, 2002 Boston College, Chestnut Hill, MA.
- Kalafat, D., Li, X., Kuleli, H.S., Toksöz, M.N. 2003. The Afyon, Turkey Earthquake: Source Characteristics and Implications for Earthquake Triggering, Geophysical Research Abstracts, Vol. 5, 13694, European Geophysical Society EGS - AGU - EUG Joint Assembly, Nice, France, April 2003.
- Kalafat, D., Yılmaz, M., Kekovalı, K., Görgün, E., Poyraz, A. S. 2009. Türkiye Deprem Ağına ait Genişbantlı (BB) Deprem İstasyonları Kullanılarak Yapılan Yakın Gerçek Zamanlı Bölgesel Moment Tensör Değerlendirmeleri – Near Real Time Regional Moment Tensor Estimation Using Turkish Seismic Network's Broadband Stations, International Earthquake Symposium, Abstracts Book p. 62, 17-19 August 2009, Kocaeli-Turkey.
- Kaya, S., Esat, K., Ecevitoglu, B., Işık, V., Kaypak, B., Aldaş, G.U., Can, Z.A., Baksı, E.E., Akkaya, İ., Seyitoğlu, G. 2014. Afyon-Akşehir Grabeni Batı Kenarının Tektonik Özellikleri Üzerine Jeolojik ve Jeofizik Gözlemler: İki Evreli Genişleme Modeli Hakkında Tartışmalara Bir Katkı (Geological and Geophysical Observations on the Tectonic Features of Western Part of the Afyon-Akşehir Graben: A Contribution to the Arguments on the Two-stage Extension Model), Hacettepe Üniversitesi Yerbilimleri Uygulama ve Araştırma Merkezi Bülteni, Yerbilimleri 35(1),1-16.
- Klein, F. W. 1985. User's guide to HYPOINVERSE, a program for VAX and Professional 350 computers to solve for earthquake locations: U.S. Geological Survey Open-File Report 85-515, 53p. <http://pubs.usgs.gov/of/1985/0515/report.pdf>
- Koçyiğit, A. 1984. Güneybatı Türkiye ve yakın dolayında levha içi iki yeni tektonik gelişim, TJK Bülteni C 27, 1-15.
- Koçyiğit, A. 1996. Lakes region graben-horst system, SW Turkey: differential stretching and commencement age of the extensional neotectonic regime. In: Görür, N. (coordinator), National Marine Geological and Geophysical Programme, Workshop-1, İstanbul, Extended Abstracts, 99-103.
- Koçyiğit, A. 2008. Orta Anadolu'nun aktif tektoniği ve jeotermal Enerji potansiyeli. Orta Doğu Teknik Üniversitesi, Müh. Fakültesi, Jeoloji Müh. Bölümü, Proje No. 07-03-09-1-00-23, Final Raporu, 135 (unpublished).
- Koçyiğit, A., Özacar, A. 2003. Extensional neotectonic regime through the NE edge of outer Isparta Angle, SW Turkey: new field and seismic data. Turkish Journal of Earth Sciences 12, 67-90.
- Koçyiğit, A., Onay, E., Saraç, G. 2000. Episodic graben formation and extensional neotectonic regime in west Central Anatolia and the Isparta Angle: A case study in the Akşehir-Afyon graben, Turkey, in E. Bozkurt, J. A. Winchester, and J. D. A. Piper (editors), Tectonics and Magmatism in Turkey and the Surrounding Area, Geological Society, London, Special Publication 173, 405-421.
- Lee, W.H.K., Lahr, J.C. 1975. HYPO71 (revised): a computer program for determining hypocenter, magnitude, and first motion pattern of local earthquakes, U.S. Geol. Surv., Open-File Rept. 75-3111, 1-113.
- Li, X., Kalafat, D., Kuleli, S., Toksöz, M. N. 2002. Complex Source Process of the February 3, 2002 Afyon Turkey Earthquake, EOS Trans. AGU 83 (47), Fall Meeting Suppl., Abstract , S71C-1111 0830h Poster, MCC: Hall C Sunday 0830h Presiding, Boston.
- Lienert, B. R., Berg, E., Frazer, L. N. 1986. HYPOCENTER: An earthquake location method using centered, scaled, and adaptively damped least squares: Bulletin of the Seismological Society of America 76, 771-783.
- NASA/USGS (<https://earthexplorer.usgs.gov/>) 30m SRTM Shuttle Radar Topography Mission (SRTM) – JPL-NASA topoğrafya verisi.
- Öğdüm, F., Kozan, T., Bircan, A., Bozbay, E. 1991. Sultandağları ile çevresindeki havzaların jeomorfolojisi ve genç tektoniği, Maden Tetkik ve Arama Genel Müdürlüğü Report no. 9123, Ankara (unpublished).
- Özgül, N., Bölükbaşı, S., Alkan, H., Öztaş, Y., Korucu, M. 1991. Göller bölgesinin Tektonik-stratigrafik birlikleri, Ozan Sungurlu Sempozyumu Bildirileri, 213-237.
- Richter, C. F. 1936. An Instrumental Earthquake Magnitude Scale, Bull Seism Soc Am 25: 1-32.
- Richter, C.F. 1948. History and Applications of the Magnitude Scale, Bur. Central Seismol Int Ser A, 17: 217-224.
- Seyitoğlu, G., Scott, B.C. 1996. The cause of N-S extensional tectonics in western Turkey: tectonic escape vs. back-arc spreading vs. orogenic collapse. Journal of Geodynamics, 22, 145-153
- Sokos, E., Zahradník, J. 2013. Evaluating Centroid Moment Tensor Uncertainty in the New Version of ISOLA Software, Seismological Research Letters 84, 4, 656-665.
- Şaroğlu, F., Emre, Ö., Boray, A. 1987. Türkiye'nin aktif fayları ve depremsellikleri, Maden Tetkik ve Arama Genel Müdürlüğü Report no. 8174, 394, Ankara (unpublished).

Şarođlu, F., Emre, Ö., Kuşçu, İ. 1992. Türkiye diri fay haritası, Maden Tetkik ve Arama Genel Müdürlüğü, Ankara, ölçek: 1/1.000.000.

Şengör, A.M.C., Görür, N., Şarođlu, F.1985. Strike-slip faulting and related basin formation in zones of tectonic escape: Turkey as a case study. The Society of Economic Paleontologists and Mineralogists, Special Publication, 37, 227-264.

Ulusay, R., Kasapođlu, E., Dirik, K., Gökçeođlu, C. 2002. 3 Şubat 2002 Sultandađı (Afyon) Depremi Saha

İnceleme Raporu, Hacettepe Üniversitesi M.F. Jeoloji Müh. Bölümü, 44, Mart 2002, Ankara (in Turkish).

Uysal, Ş. 1995. Graben formation in the collisional belts: an example from SW Anatolia, Eşençay graben. In: Pişkin, D., Ergün, M., Savaşçın, M.Y. and Tarcan, G. (eds), International Earth Science Colloquium on the Aegean Region Proceedings, 273-287.